Desalination and Water Treatment
www.deswater.com
doi: 10.5004/dwt.2022.28763

275 (2022) 81–91
November

Adsorption of copper and lead from rainwater using adsorbents based on diatomite and calcium alginate

Anna Marszałek

Silesian University of Technology, Department of Energy and Environmental Engineering, Konarskiego 18, 44-100 Gliwice, Poland, email: anna.marszalek@polsl.pl

Received 4 March 2022; Accepted 18 July 2022

ABSTRACT

Contamination of water bodies with toxic heavy metals poses significant problems in many countries. Copper and lead are harmful toxic metals found in rainwater. Readily available, economical, and environmentally friendly sorption materials are sought to remove these metals, and this study focuses on their removal. Capsules of calcium alginate combined with diatomaceous earth were prepared by mixing sodium alginate with diatomite, which was added to a calcium chloride solution. Alginate forms hydrogels in the presence of divalent cations. These materials were characterized by scanning electron microscopy, point analysis energy-dispersive X-ray spectroscopy, and measuring the surface area and pore size distribution using the Brunauer–Emmett–Teller (BET) low-temperature nitrogen adsorption and desorption technique (BET). Additional studies examined adsorption under static conditions to determine the adsorption isotherms and adsorption kinetics of copper and lead and showed high levels of both copper and lead removal. Efficiencies of 91.2% and 91.6% at a dose of 2 g/L for 2 h were achieved for copper and lead removal, respectively. The best rainwater solution results were obtained for copper at pH 6 and pH 8 for lead. Therefore, encapsulation of diatomite with alginate polymer is a solution to adsorption problems during the recovery of fine particles of diatomite from aqueous solutions.

Keywords: Adsorption, Heavy metals, Rainwater, Diatomite, Sodium alginate

1. Introduction

Diatomite is diatomaceous earth, a natural organic mineral. Silica with varying degrees of hydration and small amounts of other minerals comprise diatomite. Diatomite is relatively cheap, readily available, and widely used due to its unique properties. It exhibits interesting technological features—odorless, chemically inert, low thermal conductivity, high purity, and non-toxic [1]. Those unique properties make it widely used in filtration, which constitutes a majority of diatomite production. Diatomaceous earth is widely used as a filter medium in brewing and winemaking. The diatomite surface retains unwanted clouding compounds such as proteins, tannins, and yeast cells during filtration [2].

The sorption properties of diatomaceous earth make it useful for purification of aqueous solutions. Environmental removal of heavy metal ions remains a big problem due to health hazards associated with their toxicity and non-biodegradability [3]. Specifically, diatomite plays an important role in the elimination of water-soluble organic cationic dyes and heavy metal ion contamination [4]. Literature reviews by Sriram et al. [5] and de Namor et al. [6] discussed the removal of these contaminants in detail using diatomaceous earth or surface modified diatomaceous

Presented at the 2nd International Conference on Strategies toward Green Deal Implementation – Water, Raw Materials and Energy (ICGreenDeal2021), 8–10 December 2021, held online by the Mineral and Energy Economy Research Institute, Polish Academy of Sciences

earth, confirmed their excellent physico-chemical properties and low cost. Coagulation, adsorption, advanced oxidation, ion exchange, and membrane filtration all remove metal ions from water [7–10]. However, adsorption for water treatment has gained popularity due to its ease of operation, simplicity, speed, economy, workability, regeneration, and high efficiency. Ren et al. [4] developed a new absorbent material based on diatomaceous earth via hydrothermal modification using calcined diatomaceous earth and lime (CaO) as raw materials. They compared samples before and after modification using various analytical techniques and confirmed that hydrated calcium silicate gels and xonotlite improved the adsorption capacity and surface properties of calcined diatomaceous earth [4]. Shen et al. [11] indicated that modified diatomite (using NaOH and $MnCl_2$) was an effective cadmium wastewater adsorbent and suitable for recycling. Those results showed the removal rate of Cd(II) on modified diatomite was 98.69%, while unmodified diatomite was 58.30%. Memedi et al. [12] removed 100% of chromium ions from water using clay diatomite. Sharipova et al. [13] tried to remove triclosan from model solutions, and Hadri et al. [14] examined the adsorption of methylene blue on diatomaceous earth. Gokirmak Sogut and Caliskan [15] removed lead, copper, and cadmium ions from an aqueous solution using crude and thermally modified diatomite. ElSayed [3] observed high diatomite adsorption efficiencies for heavy metal removal that included aluminum, barium, cadmium, chromium, copper, iron, lead, manganese, nickel, and zinc. Removal efficiencies for Ba, Cd, Pb, Mn, Ni, and Zn indicated it remained unchanged during the experiment when the time increased from 15 to 70 min and recorded (99–99.7%) [3]. The individual characteristics of diatomite and sodium alginate allow their combination into an effective composite material to remove heavy metals. Studies of heavy metal adsorption using this type of composite were not found. Therefore, encapsulating diatomaceous earth with alginate has merit. Diatomaceous earth is a loose material and there are problems with its recovery from aqueous solutions, which may cause turbidity. A promising solution cross-links diatomaceous earth with calcium alginate to adsorb heavy metals. This project sought to immobilize a fine diatomaceous earth powder with calcium alginate to obtain readily separated and recovered granules. Calcium alginate beads combined with diatomaceous earth were prepared by mixing sodium alginate with diatomite and added to a calcium chloride solution. These novel granular sorbents provide a low-cost solution for heavy metal ion removal from water. This adsorption process was also examined using real rainwater.

2. Materials and methods

2.1. Rainwater characterization

Rainwater was collected in October from the roof of a house covered with steel tiles in Ruda Śląska in Poland. Dust levels in the air during this time were 38 μg/m^3; the precipitation was 49 mm. The rainwater harvesting system was equipped with a rainwater concrete tank and an Atlas Filtri FA BX filter that removed mechanical impurities such as sand, rust, silt, corrosion, turbidity, sediments, and some sparingly soluble iron compounds. A "25-μm cartridge" removed contaminants >25 μm. The samples were taken directly from the tank into a clean container and tests were conducted immediately.

The rainwater did not contain heavy metal ions therefore, was spiked with a sufficient volume of cooper and lead solution ($CuCl_2$ and $PbCl_2$) to obtain a concentration equal to 5 mg/L. The basic physico-chemical characteristics of raw rainwater are presented in Table 1.

2.2. Diatomite

Diatomite (diatomaceous earth) came from the diatomite mine in Jawornik Ruski. Diatomaceous earth samples were prepared by washing with deionized water and dried at 80°C for 12 h. The samples were ground and sieved through a 0.5 mm pneumatic screen.

2.3. Chemicals

All materials used were purchased as analytical grade reagents and used without further purification. Sodium alginate, H_2SO_4, and $CaCl_2$ were purchased from Sigma-Aldrich (Poznań, Poland). Copper ion concentrations were monitored spectrophotometrically with Merck test kits. Copper and lead standard solutions ($CuCl_2$ and $PbCl_2$) were purchased from Merck (Merck sp. z.o.o. Poland).

2.4. Sample preparation

Diatomite (12 g) was dispersed in 50 mL of deionized water and stirred. In a separate beaker, a 2% (w/v) suspension of alginate was prepared by dissolving 4 g of sodium alginate in deionized water (200 mL). A homogenized suspension of diatomite (50 mL) was added to the alginate suspension and stirred for 4 h. The mixture was transferred to a separatory funnel when it became homogeneous, then added dropwise to an aqueous coagulation bath containing 500 mL of 2% $CaCl_2$ and stirred for 3 h. The beads were filtered, washed with deionized water (4 × 200 mL), dried at room temperature for 24 h, and at 60°C in an oven. The humidity of the adsorbents was not determined. The beads were dried in an oven at 60°C before starting each stage.

2.5. Adsorbent characterization

The surface morphologies were investigated by scanning electron microscopy (SEM; JSM 6360LA, JEOL-Japan).

Table 1
Physico-chemical characteristics of rainwater

Parameter	Rainwater (average value)
pH	6.8
Conductivity, μS/cm	27.8
Color, mg Pt/L	12
Turbidity, FTU	4
COD, mg/L	105
Absorbance UV_{254}, 1/cm	0.11
TOC, mg/L	9.36

COD – Chemical oxygen demand; TOC – Total organic carbon.

An energy-dispersive X-ray spectroscopy (EDS) point analysis was also performed. The adsorbent structural properties were determined by measuring the surface areas and pore size distributions using the Brunauer–Emmett–Teller (BET) method. The functional groups on the adsorbent surface were determined using Fourier-transform infrared spectroscopy (Bruker FTIR TENSORII; 400–4,000 cm^{-1}; resolution, 1 cm^{-1}). The zeta potential was determined based on flow current measurements using a SurPAss electrokinetic analyzer (Anton Paar; Austria). Measurements were made using KCl (0.01 M) as the primary electrolyte and changes in pH during titration were made by adding HCl or NaOH (0.1 M) solutions.

2.6. Adsorption experiments

Cu(II) and Pb(II) adsorptions evaluated the adsorption capacities of encapsulated diatomite using batch experiments. The effects of contact time and dosage were investigated. Experiments were conducted in a multicomponent solution. Adsorptions were conducted in 100 mL glass flasks using a 100 mL solution at room temperature (20°C ± 2°C) in an incubator shaker at 300 rpm. The mass of the sorbents varied from 0.25–2 g/L. Kinetic experiments were conducted as follows: 1 g/L of sorbent was added to 100 mL of feed water (C_0 = 5 mg/L) in a glass flask and shaken at 300 rpm/min for 15, 30, 45, 60, 90, 120, 180, and 240 min. The pH of the solution was kept constant. Batch experiments were also conducted to study the effects of solution pH, and the pH was altered using 0.1 mol/L HNO_3/NaOH solutions. Tests to determine the effectiveness of composite beads at higher copper and lead concentrations from rainwater were conducted. Adsorption experiments were conducted using different ion concentrations in pH 6 rainwater. Each experiment was performed in duplicate and the mean value ensured quality assurance. Five regeneration and re-use cycles of alginate-diatomite beads were carried out. The beads were eluted with 0.1 M HNO_3 and rinsed with distilled water to a pH of 6.5.

The adsorption kinetics of diatomite granules were determined using pseudo-first-order and pseudo-second-order kinetic models, given in Eqs. (1) and (2) respectively [16]:

$$\ln\frac{q_e - q_t}{q_e} = -K_1 \times t \tag{1}$$

$$\frac{t}{q_t} = \frac{1}{K_2 \times g_e^2} + \frac{t}{g_e} \tag{2}$$

The experimental data were fit to a nonlinear model using pseudo-second-order kinetic equations expressed as shown in Eq. (3) [16],

$$\frac{t}{Q_t} = \frac{1}{K_2\left(Q_e\right)^2} + \frac{t}{Q_e} \tag{3}$$

where Q_e and Q_t are the amounts of micropollutants adsorbed at equilibrium and time (t), respectively, and K_2 is the pseudo-second-order rate constant.

Based on the pseudo-second-order model, the half adsorption time [$t_{1/2}$; Eq. (4)] and the initial adsorption rate [h; Eq. (5)] were calculated [16]:

$$t_{1/2} = \frac{1}{K_2 \times Q_e} \tag{4}$$

$$h = K_2 Q_e^2 \tag{5}$$

The amount adsorbed was calculated using Eq. (6):

$$Q_e = \frac{\left(C_0 - C_e\right) \times V}{m} \tag{6}$$

where Q_e (mg/g) is the equilibrium adsorbed amount, C_0 and C_e (mg/L) are the initial and equilibrium concentrations of adsorbates, respectively, m (g) is the adsorbent mass, and V (L) is the volume of the feed water.

Two common adsorption isotherm models (Langmuir and Freundlich) were used to fit the experimental data, described briefly below.

The Langmuir equation assumes monolayer adsorption, where molecules interact only with the sorbent surface, Eq. (7) [16].

$$\frac{1}{Q_e} = \frac{1}{Q_m K_L} \cdot \frac{1}{C_e} + \frac{1}{Q_m} \tag{7}$$

where Q_m (mg/g) is the maximum adsorption capacity, and K_L (L/mg) is the Langmuir fitting parameter.

The Freundlich model is empirical and adequately describes adsorption on heterogeneous surface energy systems. The model has significant importance for chemisorption and some cases of physisorption, shown in Eq. (8) [16].

$$\log q_e = \log K_F + \frac{1}{n}\log C_e \tag{8}$$

where K_F ((mg/g)(L/mg)^n) is the Freundlich adsorption coefficient, and n is the number describing surface heterogeneity and sorption intensities.

3. Results and discussion

3.1. Material structure

SEM measured the surface morphologies of the minerals and Fig. 1 shows those images.

The SEM-EDS sample shows the diatomite surface morphology, with clear cross-linking of the diatomite with sodium alginate. The granule surface is irregular. Moreover, EDS characterization data (Fig. 2 and Table 2) shows high levels of Si, O, C, and Fe, which confirm the diatomite chemical composition. The main component is amorphous silica, although it may contain organic contaminants and environmental metal oxides (MgO, Al_2O_3, Fe_2O_3) [17].

Table 3 summarizes the specific surface area and structural parameters, while Fig. 3 shows the BET sample analysis.

According to IUPAC (International Union of Pure and Applied Chemistry) classifications, the nitrogen

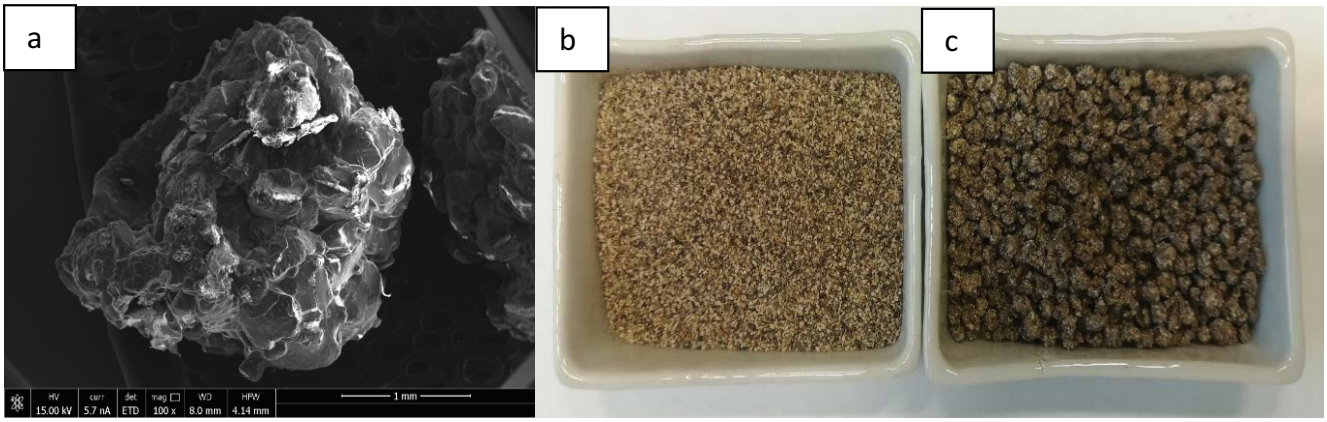

Fig. 1. SEM images of beads diatomite (a), photos of diatomite (b) and beads diatomite (c).

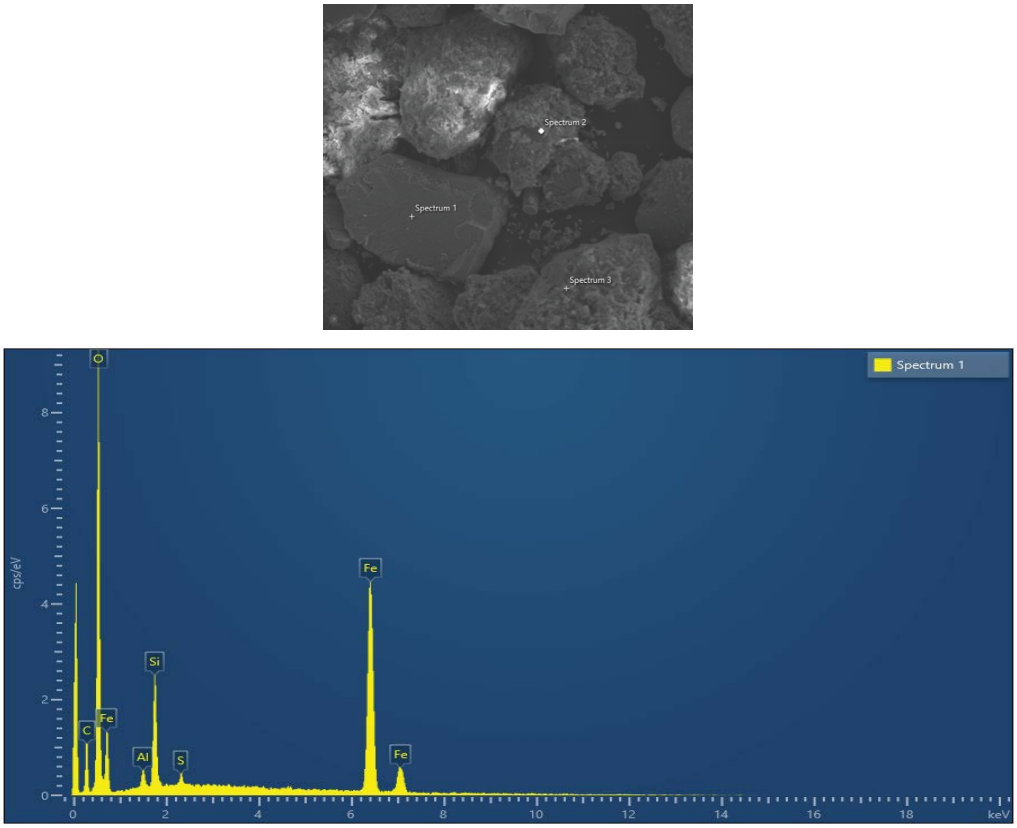

Fig. 2. EDS spectra of diatomite.

Table 2
Percentage composition of diatomite from EDS

Element (%)	C	O	Na	Mg	Al	Si	S	K	Ti	Fe
Max.	23.41	52.31	0.45	0.55	6.54	29.49	0.49	2.55	0.38	33.82
Min.	21.21	35.63	0.45	0.32	0.83	4.86	0.49	0.49	0.13	1.22
Average	22.13	42.06			3.73	17.32				12.98
Standard deviation	1.15	8.97			2.85	12.32				18.10

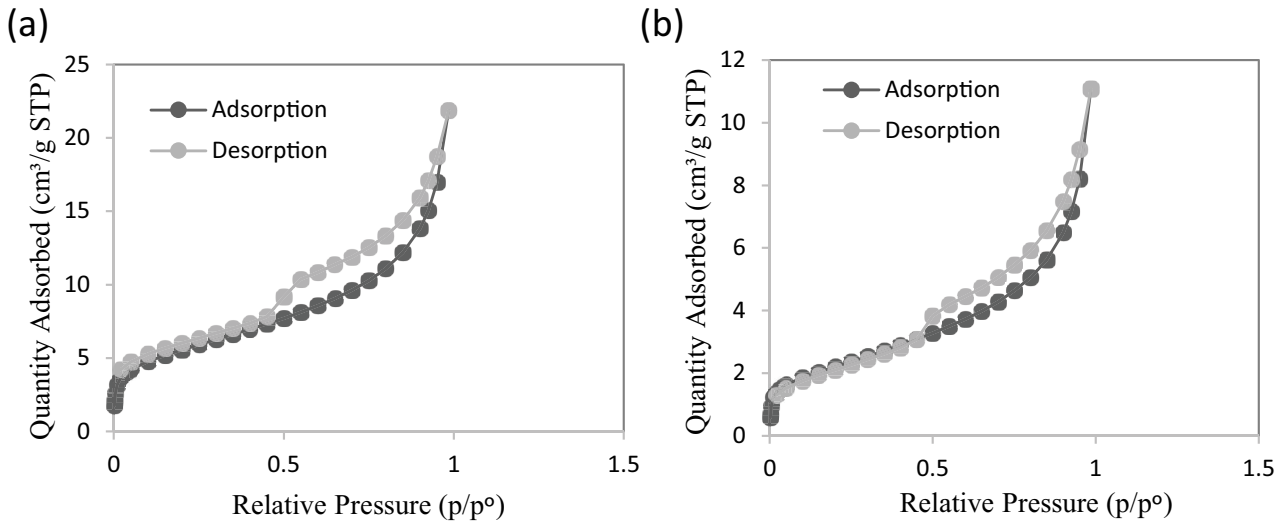

Fig. 3. N_2 adsorption–desorption curves of (a) diatomite and (b) beads of diatomite.

adsorption and desorption isotherms were Type II with an H3 hysteresis loop. The BET area for diatomite was 19.72 and 7.936 m^2/g for encapsulated diatomite. FTIR determined the functional group nature of the test sample, shown in Fig. 4.

The wide band from 3,402–3,112 cm^{-1} indicates –OH groups from water. The characteristic band from 2,300–2,400 cm^{-1} indicated the presence of atmospheric carbon dioxide [18]. The many peaks and wide band from 900–1,100 cm^{-1} were attributed to water (air humidity band characteristic of the –OH group in water). The peak at 1,601 cm^{-1} stems from alginate and confirmed a C=O [19]. An asymmetric band at 1,422 cm^{-1} was assigned to COO– group oscillation and indicated the presence of carboxyl groups in alginate. That band indicated the sorbent contained carboxyl groups derived from sodium alginate [19]. The peak at 997 cm^{-1} was related to Si–O–Si siloxane bond vibrations.

3.2. Effect of adsorbent dose on removal percentage

The dose effects of diatomite from 0.025–0.2 g/L at 25°C were investigated (Fig. 5). The metal ion concentration was 5 mg/L and the contact time was 2 h. The efficiency of copper and lead removal increased from 40% to 91% for Cu(II) and from 71% to 91% for Pb(II) as the adsorbent increased from 0.5 to 2 g/L. At low diatomite levels, all surface sites are exposed to metal ions, which led to rapid saturation and the highest saturation at 2 g/L of diatomaceous earth for both metals. The adsorbent dose was important as it determined the adsorbent capacity for a given initial adsorbate concentration and many studies confirmed these results [20]. Adsorption stabilized above 0.1 g/L, and similar results were reported [21] for Cr and Fe removal on kaolinite.

3.3. Effect of pH

The adsorption capacities of heavy metals on the adsorbent surface were measured by controlling the pH at 25°C was investigated (Fig. 6).

A slow metal uptake was noted at low pH by the diatomite and explained by surface site positive charge increases. Increasing the solution pH increased the number of active sites (the number of anionic charges on alginate composites) available for interaction with metal ions. Sorption increased with pH, at low pH, sorption functional group stability was limited (protonated form –COOH) and adsorption of divalent metals to alginate normally occurred due to ion exchange involving alginate carboxyl groups [19]. However, lead removal increased when the pH increased from 6 to 8.0, though the best results for copper were obtained at pH 6.0. Bilgin and Tulun [22] showed a good ability to remove lead(II) by diatomite at a pH from 4–6 and established an optimal adsorption pH of 6. The adsorption selectivity was Pb > Cu, regardless of pH, due to the correlation of heavy metal ionic radii with the outer and inner pore diameters of the diatomite. The diatomite selectivity results against the tested metals agreed with studies by ElSayed [3]. Alginate-diatomite beads have a positive charge and zeta potential of 21.3 mV at a rainwater pH of 6.8. One of the main mechanisms of heavy metal ion adsorption on the surface of the tested adsorbent was ion exchange, which takes place between heavy metals and cross-linking cations (Ca^{2+}). Ion exchange also occurs with protons on oxygen-containing functional groups such as carboxyl and hydroxyl groups on alginate. The metal ion size and chemistry of the adsorbent surface functional groups significantly influenced ion exchange efficiency during heavy metal adsorption [23].

3.4. Influence of Cu(II) and Pb(II) concertation in rainwater

A significant reduction in the adsorption efficiency for copper was found based on the initial lead and copper concentrations in rainwater. The lead adsorption efficiency decreased slightly, from 75% to 65% with lead concentrations from 10–50 mg/L. On the other hand, the copper adsorption efficiency for the same adsorbate concentrations decreased significantly, from 44%–5%. Fig. 7 shows those results.

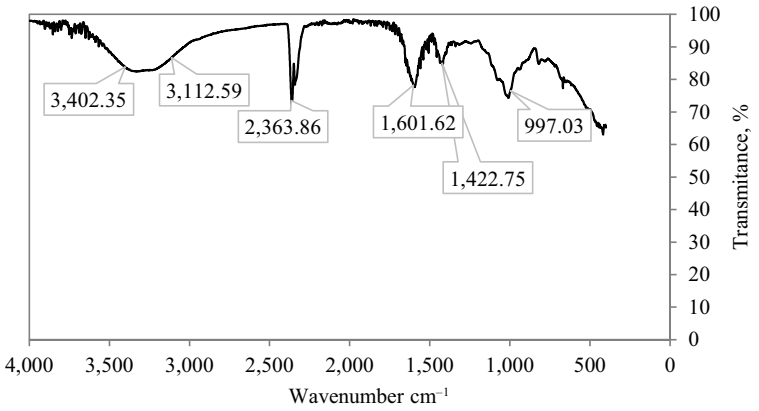

Fig. 4. FTIR spectrum of diatomite-alginate beads.

Table 3
Characteristics of diatomite and diatomite beads from nitrogen sorption–desorption measurements

Adsorbent	Specific surface area (SSA), (m^2/g)	Total volume in pores, (cm^3/g)	Pore size, (nm)
Diatomite	19.7296	0.0415	1.852
Beads diatomite	7.936	0.0208	1.841

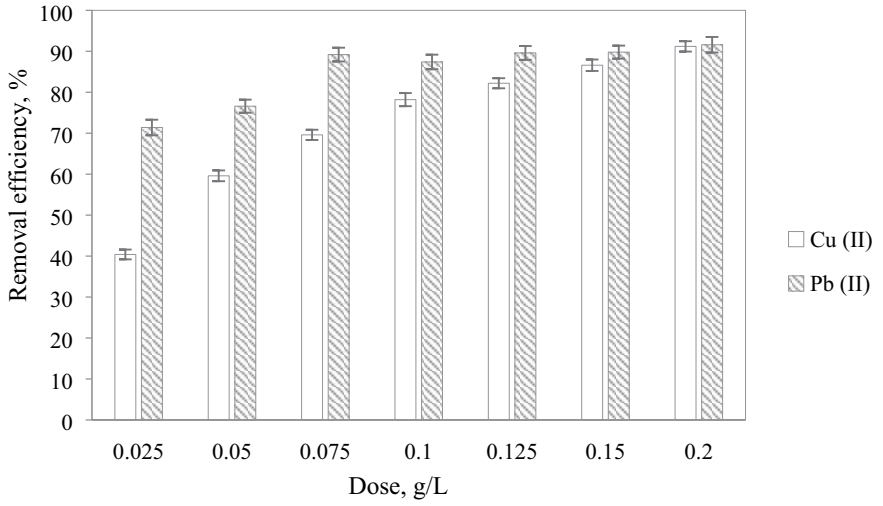

Fig. 5. Effect of sorbent dose on Cu(II) and Pb(II) concentration in rainwater (C_0 = 5 mg/L). Error bars: standard deviation.

3.5. Adsorption isotherms of Cu(II) and Pb(II)

The equilibrium data obtained for adsorptions of copper and lead by diatomite beads were analyzed using Langmuir and Freundlich models. The Langmuir model (Fig. 8) fit the experimental data better than the Freundlich model. The Langmuir model is the most widely used isothermal model, assumes adsorption is limited to one molecular layer, all adsorption sites on the surface are energetically identical, and there is no interaction between the adsorbate molecules [22]. Table 4 gives the Freundlich and Langmuir parameters, equations, and the correlation coefficients for Cu(II) adsorption on the sorbents.

The Langmuir adsorption model showed the maximum adsorption capacity for capsules based on diatomite and sodium alginate was 9.93 mg/g for Cu and 17.3 mg/g for Pb. Bilgin and Tulun [22] determined a maximum lead adsorption capacity of 56.49 mg/g using the Langmuir adsorption isotherm. On the other hand, Pawar et al. [25] investigated bentonite-alginate composites to remove copper and lead, reported maximum Langmuir sorption capacities of 17.30 and 107.52 mg/g for Cu(II) and Pb(II), respectively. He found a sorption capacity for lead 6.21 times higher than cooper. For diatomite-alginate beads, the adsorption capacity was twice as high.

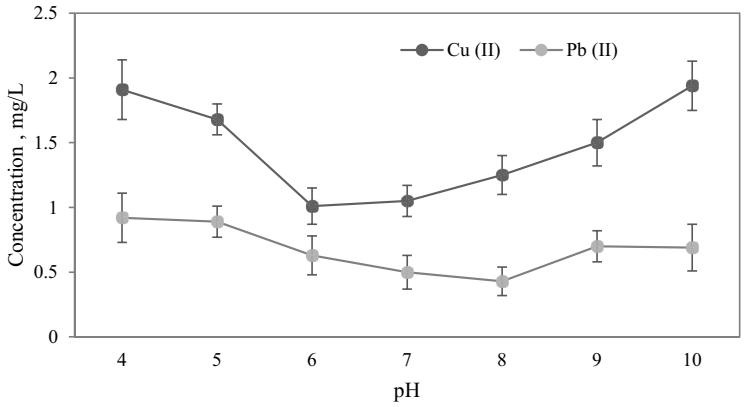

Fig. 6. Influence of rainwater pH on Cu(II) and Pb(II) adsorption.

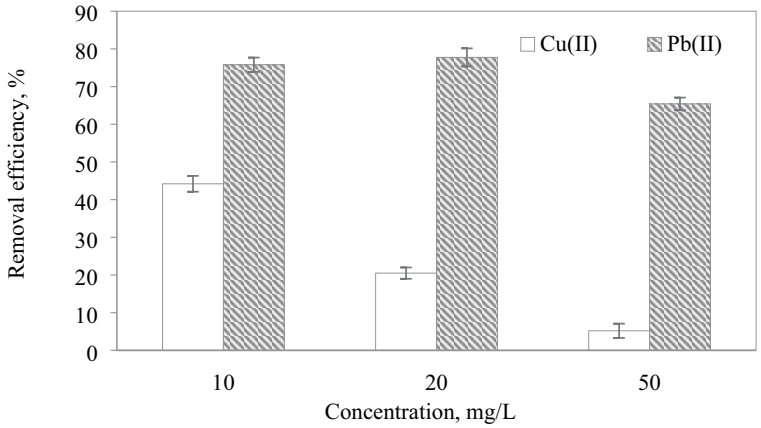

Fig. 7. Cu(II) and Pb(II) removal based on rainwater concentrations. Error bars: standard deviation.

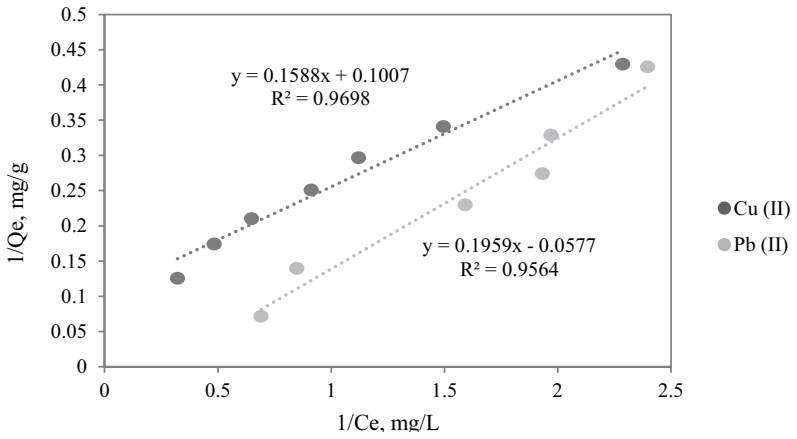

Fig. 8. Langmuir isotherms of Cu(II) on diatomite beads.

Zhao et al. prepared an adsorbent of cellulose nanofibers and sodium alginate to remove lead from water [26]. This adsorbent was effective and the Q_m fit from the Langmuir model was 318.47 mg/g. As shown in the adsorbent dependence, the feed solution or metal concentration resulted in a very different adsorption capacity. It is also important that tests are carried out on real solutions [22].

3.6. Adsorption kinetics of Cu(II) and Pb(II)

Contact time is an important factor that influences heavy metal ion adsorption on diatomaceous earth. A batch experiment investigated the effect of contact time on the interaction between diatomite particles and metal ions. Maximum adsorption capacities, Q_e, K_1, K_2, and correlation coefficients

Table 4
Freundlich and Langmuir equation parameters, and correlation coefficients for Cu(II) adsorption on the sorbents

Adsorbent	Langmuir			Freundlich		
	Q_m (mg/g)	K_L (L/mg)	R^2 (–)	K_F ((mg/g)(L/mg)^n)	n (–)	R^2 (–)
Cu(II)	9.930	0.634	0.969	3.703	1.541	0.990
Pb(II)	17.331	0.294	0.956	7.860	0.827	0.816

Table 5
Parameters for adsorption pseudo-first-order and pseudo-second-order kinetic models

Adsorbate	Pseudo-first-order equation parameters			Pseudo-second-order equation parameters		
	K_1 (1/min)	Q_e (mg/g)	R^2	K_2 (g/(mg min))	Q_e (mg/g)	R^2
Cu(II)	0.0218	3.14	0.86	0.011	4.34	0.98
Pb(II)	0.0132	9.72	0.92	0.019	4.76	0.99

Table 6
Parameters for the pseudo-second-order kinetic model for Pb(II) and Cu(II) adsorption

Adsorbate	Pseudo-second-order equation parameters					
	K_2 (g/(mg min))	$Q_{t(\exp)}$ (mg/g)	$Q_{t(\text{cal})}$ (mg/g)	$t_{1/2}$ (min)	h (mg/(g min))	R^2
Cu(II)	0.0109	4.227	3.929	0.0464	0.2	0.957
Pb(II)	0.0545	4.166	4.256	0.227	0.95	0.972

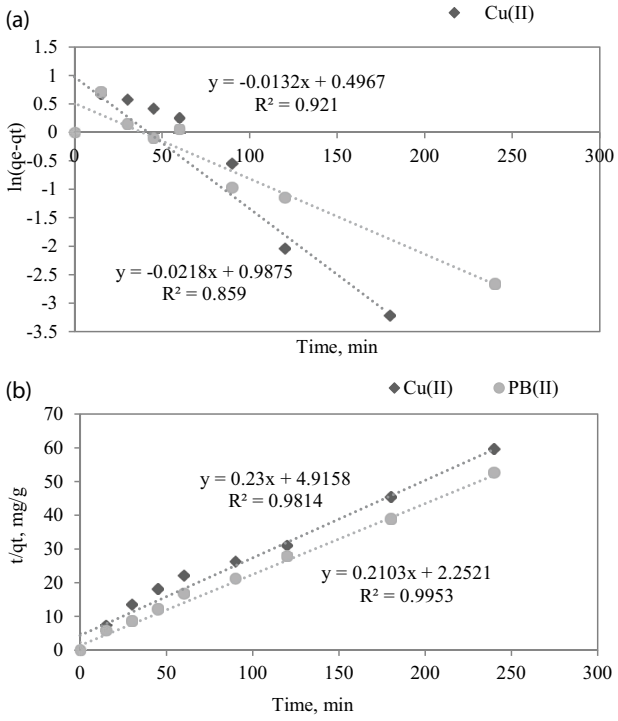

Fig. 9. Adsorption kinetic curves of Cu(II) and Pb(II) by pseudo-first-order (A) and pseudo-second-order kinetics (B).

R^2, were calculated based on pseudo-first-order and pseudo-second-order models and presented in Table 5. R^2 values for the pseudo-second-order model exceeded the pseudo-first-order model (Fig. 9).

The pseudo-second-order model described the adsorption of heavy metals; Table 6 gives those parameters. The calculated (Q_(t(cal))) values agreed with experimental data (Q_(t(exp))), which suggested the adsorption followed second-order kinetics and was used to determine the corresponding kinetic parameters. Pb adsorption was the most rapid based on those parameters, which indicated $t_{(1/2)}$, h, and K_2, were higher for Pb than for Cu.

These results indicated that copper and lead adsorption occurred quickly but declined, readily explained by the large surface area of the diatomite ready to interact with heavy metals. Equilibrium occurred within 90 min. The adsorption time and the dose confirmed lead was removed before copper and this result agreed with previous literature reports. Selectivity could be due to the metal electronegativities. A comparison of the electronegativity of the tested metals is not entirely true for the above hypothesis Pb(II) (2.33) > Cu(II) (1.9). This is probably the reason for the faster adsorption of lead compared to other metals [25].

3.7. Desorption studies

The practical application of regeneration and repeatability is the fundamental study of the use of an adsorbent.

Table 7
Effectiveness of alginate-based adsorbents

Type of adsorbent	Metal	Degree of absorption	References
Chitosan immobilized in alginate	Cu, Cd	81%, 87%	[19]
Industrial waste encapsulated cryogenic alginate beads	Pb, Cd	72%, 50%	[27]
Succinate (SBS)/alginate (Alg.) (SAPGB)	Pb, Cd	90%, 90%	[28]
Sodium alginate/carboxymethyl chitosan hydrogel beads	Cu	82%	[29]
Alginate-immobilized bentonite	Cu	94%	[30]
Activated bentonite-alginate composite beads	Cu, Pb	72%, 96%	[25]
Nanostructured calcium alginate hydrogel	Cu, Cd	87%, 69%	[31]
Magnetic bentonite/carboxymethyl chitosan/sodium alginate hydrogel beads	Cu	93%	[32]
Carboxylated chitosan/carboxylated nanocellulose hydrogel beads	Pb	96%	[33]
Alginate (AL)-based composite beads filled with bentonite (BE) and phosphate washing sludge (PS)	Pb	95%	[34]

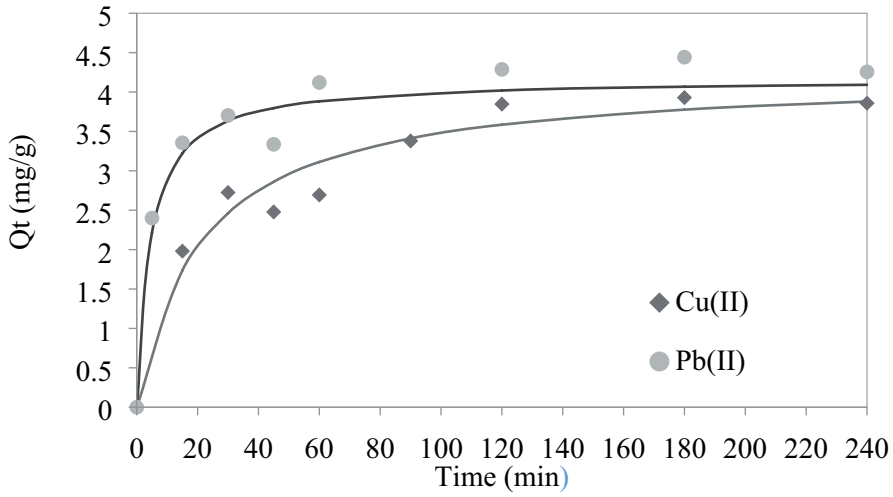

Fig. 10. Adsorption kinetic curves of Cu(II) and Pb(II) by pseudo-second-order kinetics.

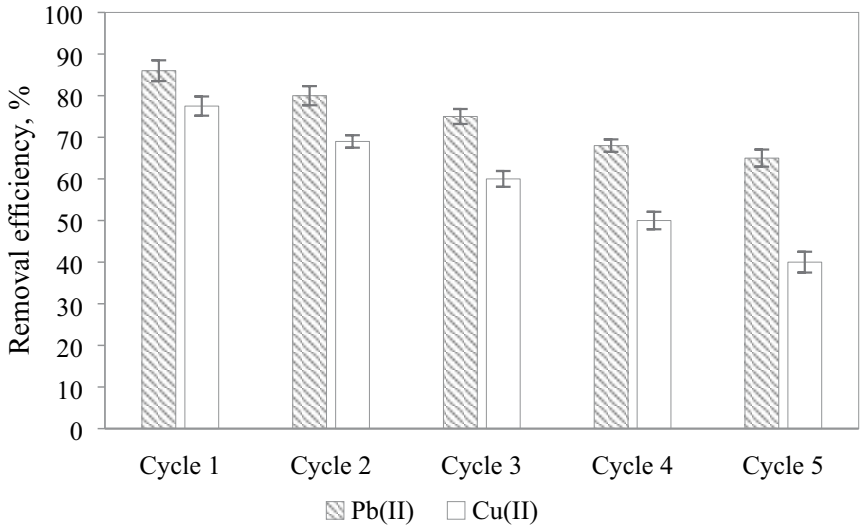

Fig. 11. Degree of Pb(II) and Cu(II) removal after successive desorption cycles.

A regeneration/re-use of the alginate-diatomite beads was conducted, which showed high desorption upon adsorption of Pb(II) and Cu(II) ions from rainwater. The beads were eluted with 0.1 M HNO_3 and rinsed with distilled water to a pH of 6.5. Five cycles were performed, and the percentages of lead and copper removal in successive desorption cycles are shown in Fig. 11.

3.8. Comparison of heavy metal adsorption capacity by other calcium alginate-based adsorbents

Alginate-based beads adsorb heavy metals very well. Previous literature reports suggested that alginate may be present and modified in various combinations. Several groups emphasized the synthesis of sodium alginate composite materials to improve heavy metal adsorption. Table 7 shows the selected composites and heavy metal removal efficacies.

4. Conclusions

Adsorption showed high levels of both copper and lead removal. Removal efficiencies of 91.2% and 91.6% for Cu and Fe, respectively, were observed for 2 g/L doses and an adsorption time of 2 h. The best rainwater results were obtained for copper at pH 6 and lead at pH 8. Initial adsorption occurred quickly, then slowed, due to the initial large surface of the diatomite. Equilibrium took 90 min, and encapsulation of diatomite with a sodium alginate polymer may solve problems during adsorption with the recovery of fine particles of diatomite from aqueous solutions. The composite based on alginate and diatomite is a promising adsorbent for removing metal ions from rainwater due to its favorable sorption efficiency, low economic cost, easy synthesis, and excellent regeneration and recycling possibilities.

Acknowledgments

This research was funded by the Polish Ministry of Science and Higher Education (BKM-680/RIE4/2022).

References

[1] M. Lutyński, P. Sakiewicz, S. Lutyńska, Characterization of diatomaceous earth and halloysite resources of Poland, Minerals, 9 (2019) 670, doi: 10.3390/min9110670.
[2] X. Gong, W. Tian, L. Wang, J. Bai, K. Qiao, J. Zhao, Biological regeneration of brewery spent diatomite and its reuse in basic dye and chromium(III) ions removal, Process Saf. Environ. Prot., 128 (2019) 353–361.
[3] E.E. ElSayed, Natural diatomite as an effective adsorbent for heavy metals in water and wastewater treatment (a batch study), Water Sci., 32 (2018) 32–43.
[4] Z. Ren, Y. He, R. Zheng, Z. Guo, H. Gao, X. He, F. Wu, X. Ji, The preparation and characterization of calcined diatomite with high adsorption properties by CaO hydrothermal activation, Colloids Surf., A, 636 (2022) 128134, doi: 10.1016/j.colsurfa.2021.128134.
[5] G. Sriram, M. Kigga, U.T. Uthappa, R.M. Rego, V. Thendral, T. Kumeria, H.-Y. Jung, M.D. Kurkuri, Naturally available diatomite and their surface modification for the removal of hazardous dye and metal ions: a review, Adv. Colloid Interface Sci., 282 (2020) 102198, doi: 10.1016/j.cis.2020.102198.
[6] A.F.D. de Namor, A. El Gamouz, S. Frangie, V. Martinez, L. Valiente, O.A. Webb, Turning the volume down on heavy metals using tuned diatomite. A review of diatomite and modified diatomite for the extraction of heavy metals from water, J. Hazard. Mater., 241 (2012) 14–31.
[7] J. Du, B. Zhang, J. Li, B. Lai, Decontamination of heavy metal complexes by advanced oxidation processes: a review, Chin. Chem. Lett., 31 (2020) 2575–2582.
[8] Z. Liao, Z. Zhao, J. Zhu, H. Chen, D. Meng, Complexing characteristics between Cu(II) ions and dissolved organic matter in combined sewer overflows: implications for the removal of heavy metals by enhanced coagulation, Chemosphere, 265 (2021) 129023, doi: 10.1016/j.chemosphere.2020.129023.
[9] M. Peydayesh, T. Mohammadi, S.K. Nikouzad, A positively charged composite loose nanofiltration membrane for water purification from heavy metals, J. Membr. Sci., 611 (2020) 118205, doi: 10.1016/j.memsci.2020.118205.
[10] Q. Yang, Y. Xie, B. Zhu, Y. Zeng, H. Zhou, P. Ai, G. Chen, Positively charged PVC ultrafiltration membrane via micellar enhanced ultrafiltration for removing trace heavy metal cations, J. Water Process Eng., 46 (2022) 102552, doi: 10.1016/j.jwpe.2021.102552.
[11] T.M. Shen, H. Xu, Y. Miao, L.L. Ma, N.C. Chen, Q.L. Xie, Study on the adsorption process of Cd(II) by Mn-diatomite modified adsorbent, Mater. Lett., 300 (2021) 130087, doi: 10.1016/j.matlet.2021.130087.
[12] H. Memedi, A.A. Reka, S. Kuvendziev, K. Atkovska, M. Garai, M. Marinkovski, B. Pavlovski, K. Lisichkov, Chapter 3 – Adsorption of Cr(VI) Ions From Aqueous Solutions by Diatomite and Clayey Diatomite, S. Kumar, M.Z. Hashmi, Eds., Biological Approaches to Controlling Pollutants: Advances in Pollution Research, Woodhead Publishing, 2022, pp. 29–48. Available at: https://doi.org/10.1016/B978-0-12-824316-9.00002-1
[13] A.A. Sharipova, S.B. Aidarova, N.Y. Bekturganova, A. Tleuova, A.M. Kerimkulova, O. Yessimova, T. Kairaliyeva, O. Lygina, S. Lyubchik, R. Miller, Triclosan adsorption from model system by mineral sorbent diatomite, Colloids Surf., A, 532 (2017) 97–101.
[14] M. Hadri, Z. Chaouki, K. Draoui, M. Nawdali, A. Barhoun, H. Valdes, N. Drouiche, H. Zaitan, Adsorption of a cationic dye from aqueous solution using low-cost Moroccan diatomite: adsorption equilibrium, kinetic and thermodynamic studies, Desal. Water Treat., 75 (2017) 213–224.
[15] E. Gokirmak Sogut, N. Caliskan, Removal of lead, copper and cadmium ions from aqueous solution using raw and thermally modified diatomite, Desal. Water Treat., 58 (2017) 154–167.
[16] A. Marszałek, G. Kamińska, N. Fathy Abdel Salam, Simultaneous adsorption of organic and inorganic micropollutants from rainwater by bentonite and bentonite-carbon nanotubes composites, J. Water Process Eng., 46 (2022) 102550, doi: 10.1016/j.jwpe.2021.102550.
[17] I. Cacciotti, M. Rinaldi, J. Fabbrizi, F. Nanni, Innovative polyetherimide and diatomite based composites: influence of the diatomite kind and treatment, J. Mater. Res. Technol., 8 (2019) 1737–1745.
[18] S. Thakur, A. Verma, P. Raizada, O. Gunduz, D. Janas, W.F. Alsanie, F. Scarpa, V.K. Thakur, Bentonite-based sodium alginate/dextrin cross-linked poly(acrylic acid) hydrogel nanohybrids for facile removal of paraquat herbicide from aqueous solutions, Chemosphere, 291 (2022) 133002, doi: 10.1016/j.chemosphere.2021.133002.
[19] M. Kuczajowska-Zadrożna, U. Filipkowska, T. Jóźwiak, Adsorption of Cu(II) and Cd(II) from aqueous solutions by chitosan immobilized in alginate beads, J. Environ. Chem. Eng., 8 (2020) 103878, doi: 10.1016/j.jece.2020.103878.
[20] S. Mnasri-Ghnimi, N. Frini-Srasra, Removal of heavy metals from aqueous solutions by adsorption using single and mixed pillared clays, Appl. Clay Sci., 179 (2019) 105151, doi: 10.1016/j.clay.2019.105151.
[21] P.E. Dim, L.S. Mustapha, M. Termtanun, J.O. Okafor, Adsorption of chromium(VI) and iron(III) ions onto acid-modified kaolinite: isotherm, kinetics and thermodynamics studies, Arabian J. Chem., 14 (2021) 103064, doi: 10.1016/j.arabjc.2021.103064.

[22] M. Bilgin, Ş. Tulun, Use of diatomite for the removal of lead ions from water: thermodynamics and kinetics, Biotechnol. Biotechnol. Equip., 29 (2015) 696–704.
[23] Z.A. Sutirman, M.M. Sanagi, W.I. Wan Aini, Alginate-based adsorbents for removal of metal ions and radionuclides from aqueous solutions: a review, Int. J. Biol. Macromol., 174 (2021) 216–228.
[24] A.K. Thakur, M. Kumar, Efficacy of green alginate beads for multi-metal removal from aqueous solution, Case Stud. Chem. Environ. Eng., 3 (2021) 100100, doi: 10.1016/j.cscee.2021.100100.
[25] R.R. Pawar, L.P.G. Ingole, LS. Lee, Use of activated bentonite-alginate composite beads for efficient removal of toxic Cu^{2+} and Pb^{2+} ions from aquatic environment, Int. J. Biol. Macromol., 164 (2020) 3145–3154.
[26] H. Zhao, X. Ouyang, L. Yang, Adsorption of lead ions from aqueous solutions by porous cellulose nanofiber–sodium alginate hydrogel beads, J. Mol. Liq., 324 (2021) 115122, doi: 10.1016/j.molliq.2020.115122.
[27] A.A. Alqadami, M.A. Khan, M.R. Siddiqui, Z.A. Alothman, S. Sumbul, A facile approach to develop industrial waste encapsulated cryogenic alginate beads to sequester toxic bivalent heavy metals, J. King Saud Univ. – Sci., 32 (2020) 1444–1450.
[28] S. Fan, J. Zhou, Y. Zhang, Z. Feng, H. Hu, Z. Huang, Y. Qin, Preparation of sugarcane bagasse succinate/alginate porous gel beads via a self-assembly strategy: improving the structural stability and adsorption efficiency for heavy metal ions, Bioresour. Technol., 306 (2020) 123128, doi: 10.1016/j.biortech.2020.123128.
[29] H. Huang, Q. Yang, L. Zhang, C. Huang, Y. Liang, Polyacrylamide modified kaolin enhances adsorption of sodium alginate/carboxymethyl chitosan hydrogel beads for copper ions, Chem. Eng. Res. Des., 180 (2022) 296–305.
[30] W.S. Tan, A.S.Y. Ting, Alginate-immobilized bentonite clay: adsorption efficacy and reusability for Cu(II) removal from aqueous solution, Bioresour. Technol., 60 (2014) 115–118.
[31] X. Tao, S. Wang, Z. Li, S. Zhou, Green synthesis of network nanostructured calcium alginate hydrogel and its removal performance of Cd^{2+} and Cu^{2+} ions, Mater. Chem. Phys., 258 (2021) 123931, doi: 10.1016/j.matchemphys.2020.123931.
[32] H. Zhang, A.M. Omer, Z. Hu, L. Yang, Ch. Ji, X. Ouyang, Fabrication of magnetic bentonite/carboxymethyl chitosan/sodium alginate hydrogel beads for Cu(II) adsorption, Int. J. Biol. Macromol., 135 (2019) 490–500.
[33] X. Xu, X. Ouyang, L. Yang, Adsorption of Pb(II) from aqueous solutions using crosslinked carboxylated chitosan/carboxylated nanocellulose hydrogel beads, J. Mol. Liq., 322 (202) 114523, doi: 10.1016/j.molliq.2020.114523.
[34] I. Ayouch, I. Barrak, Z. Kassab, M. El Achaby, A. Barhoun, K. Draoui, Improved recovery of cadmium from aqueous medium by alginate composite beads filled by bentonite and phosphate washing sludge, Colloids Surf., A, 604 (2020) 125305, doi: 10.1016/j.colsurfa.2020.125305.